Journal of Food Engineering 100 (2010) 1–11

Contents lists available at ScienceDirect

Journal of Food Engineering

journal homepage: www.elsevier.com/locate/jfoodeng

Prediction of cooking times and weight losses during meat roasting

Sandro M. Goñi [a,b,c], Viviana O. Salvadori [a,c,*]

[a] Centro de Investigación y Desarrollo en Criotecnología de Alimentos (CIDCA, CONICET-La Plata), Fac. de Cs. Exactas – UNLP, 47 y 116, B1900AJJ La Plata, Argentina
[b] Departamento de Ciencia y Tecnología, UNQ, R.S. Peña 352, B1876BXD Bernal, Argentina
[c] MODIAL, Área Deptal. Ing. Qca., Fac. de Ingeniería, UNLP, 1 y 47, B1900TAG La Plata, Argentina

ARTICLE INFO

Article history:
Received 22 September 2009
Received in revised form 19 February 2010
Accepted 13 March 2010
Available online 19 March 2010

Keywords:
Meat cooking
Simulation
Dripping loss
Evaporative loss

ABSTRACT

In this work, a meat oven cooking model is developed, and its ability to predict three main process variables – evaporative loss, dripping loss and cooking time – is evaluated. Heat transfer is modelled by Fourier's law, while the internal moisture content variation is modelled as a function of water demand, which depends on the water holding capacity of beef. Experimental cooking of *semitendinosus* muscle samples was carried out in a convective oven to obtain general information about the process and to assess the model accuracy. Simulations were done by means of the finite element method, using three-dimensional irregular geometries as simulation domains. The model predictions were in good agreement with the experimental ones; the average absolute relative error was 3.91% for cooking time prediction, and 7.96% for total weight loss prediction.

1. Introduction

Oven cooking (or roasting) of meat is a food operation that affects both quality attributes and microbiological safety of processed products. In spite of the increasing importance of industrial cooking, several aspects related to this process have not been sufficiently explored. From a physical point of view, oven cooking involves heat transfer from the surrounding ambient to the food surface, and consequently induces a temperature gradient inside the product which results in an increase of internal temperature. In addition, a significant decrease of food weight is often observed during the process, which is generally attributed to water loss, neglecting other food components (i.e. proteins, lipids) losses. Internal transport of liquid water is due to thermal protein denaturation which causes the shrinkage of the meat fibres network, resulting in a mechanical force that expels the excess interstitial water towards the surface (Godsalve et al., 1977). Depending on heat and mass transfer conditions at surface, this expelled liquid water can be lost by evaporation or dripping.

Regarding the mathematical modelling of meat oven cooking, different models have been proposed depending on the assumptions about internal heat and mass transfer mechanisms. A first approach is to consider internal heat transfer occurring by conduction (Fourier's law) while neglecting internal mass transfer; then, weight loss is computed by establishing an evaporative flux at the surface. In this sense, several authors have studied different meat products, i.e. beef (Goñi et al., 2008b; Obuz et al., 2002, 2004; Singh et al., 1984; Townsend et al., 1989a,b), whole unstuffed turkeys (Chang et al., 1998). Goñi et al. (2008b) and Obuz et al. (2002) found that the average error between predicted and experimental weight losses is 20–22%. Recently, Bottani and Volpi (2009) simulated cooking of beef and turkey samples in industrial steam ovens. As cooking was performed in an oven with steam injection, the effect of water vapourization was neglected in the energy balance. Their experimental measurements indicated that also in this cooking condition, weight losses ranged from 15% to 18%. The exhaustive analysis of these reported works indicates that this model will generally fail to predict total weight loss because the liquid water loss by dripping is neglected.

Other researchers incorporated the inner mass transfer by means of the Fick's law in the mathematical model; cooking of meatballs (Huang and Mittal, 1995) and chicken patties (Chen et al., 1999) were studied on this concept. This approach can be useful to predict total weight loss in elaborated meat products, formulated with other ingredients that reduce drip losses (i.e. food additives that retain water during cooking). For raw beef, unrealistic large diffusion coefficients are needed in order to predict total weight loss (Burfoot and Self, 1989). Recently, van der Sman (2007a,b) proposed a mathematical model for meat cooking by using the Darcy's law to describe the water flux through the fibres. His work is in good agreement with the commonly accepted description of liquid water transport stated by Godsalve et al. (1977). This approach can predict both evaporative and dripping losses, though the resulting model is complex (involving

* Corresponding author at: Centro de Investigación y Desarrollo en Criotecnología de Alimentos (CIDCA, CONICET-La Plata), Fac. de Cs. Exactas – UNLP, 47 y 116, B1900AJJ La Plata, Argentina. Tel./fax: +54 221 425 4853.
E-mail address: vosalvad@ing.unlp.edu.ar (V.O. Salvadori).

0260-8774/$ - see front matter © 2010 Elsevier Ltd. All rights reserved.
doi:10.1016/j.jfoodeng.2010.03.016

Nomenclature

a_1, a_2, a_3, T_R	parameters of Eq. (14)
a_w	water activity
c	moisture content, dry basis
c_{wb}	moisture content, wet basis
$\bar{C}$	average moisture content, dry basis
C_P	specific heat of meat (J kg^{-1} K^{-1})
DL	dripping weight loss (kg)
EL	evaporative weight loss (kg)
h	convective heat transfer coefficient (W m^{-2} K^{-1})
k	thermal conductivity of meat (W m^{-1} K^{-1})
k_g	mass transfer coefficient (kg Pa^{-1} m^{-2} s^{-1})
K_W	parameters of Eq. (4), kg dry solid (s^{-1})
m_s	dry solid mass (kg)
P_{sat}	water vapour pressure (Pa)
RH	oven relative humidity
SD	standard deviation
T	temperature (°C)
WHC	water holding capacity, dry basis

Greek symbols

ε	beef emissivity
ϕ_w	volumetric fraction of water
λ	latent heat of evaporation (J kg^{-1})
ρ	meat density (kg m^{-3})
σ	Stefan–Boltzmann constant (5.67×10^{-8} W m^{-2} K^{-4})
Γ	surface of geometric model
Ω	domain of geometric model

Subscripts

exp	experimental
i	initial
o	oven
s	surface
sim	simulated

parameters difficult to estimate or either unavailable values for some properties).

This work is part of a comprehensive study on meat cooking, where the general aim is the multi-objective optimization of the process. In this way, the specific objective of this work was to develop an accurate cooking model, which allows the estimation of cooking times and also both evaporative and dripping losses. Besides, such model should be as simple as possible in terms of computational cost involved in numerical simulation, bearing in mind the ultimate optimization. The proposed mathematical model was validated by comparing its predicted results with experimental data of cooking time and weight loss.

2. Beef cooking modelling

In general, oven cooking involves heat transfer by convection and radiation from the surrounding ambient to the food surface. Then, the high surface temperature induces conductive heat transfer towards the core of the product. For modelling purposes, meat can be considered as a solid matrix composed principally by proteins and liquid water. Therefore, a simple mathematical model that describes heat transfer is expressed in the below equation:

$$\rho C_P \frac{\partial T}{\partial t} = \nabla(k \nabla T) \tag{1}$$

Due to high ambient temperature that largely surpasses 100 °C, the surface of meat rapidly achieves temperature values near 100 °C. As a result, a significant fraction of liquid water is evaporated, which can be quantified as a water vapour flux transferred to the oven ambient, j_{evap}. The heat associated to evaporative flux is added in the boundary condition for the energy balance, Eq. (2). As well, this mass flux depends on the water activity of food surface and the relative humidity of the oven ambient (Eq. (3)).

$$-nk\nabla T = h(T_s - T_o) + \varepsilon\sigma(T_s^4 - T_o^4) + \lambda j_{evap} \tag{2}$$

$$j_{evap} = k_g(a_w P_{sat}(T_s) - RHP_{sat}(T_o)) \tag{3}$$

Besides the water loss produced by superficial evaporation, there exist enough experimental evidence to say that the protein matrix acts like a sponge, which losses a significant amount of liquid water by dripping when receiving several stimuli (e.g. stress–strain due to protein denaturation, pre-processing mechanical cuts) (Tornberg, 2005). For high values of the heat and mass transfer coefficients, free liquid water can evaporate. Therefore, in these situations, total weight loss is mostly evaporative, and this model offers acceptable results. Conversely, as it does not take into account the dripping phenomena, the total weight loss will be notoriously underestimated when the heat and mass transfer coefficients present low or moderate values (Goñi et al., 2008b; Obuz et al., 2002), which is common in domestic and also in some industrial ovens. In consequence, Eq. (4) is coupled to the previous ones in order to evaluate the variation of liquid water content in the meat.

$$m_s \frac{dc}{dt} = -K_W(c - WHC(T)) \tag{4}$$

This balance establishes that water content variation is directly proportional to water demand. The water demand is the difference between the instant water content and an equilibrium value, equal to the water holding capacity (WHC). At this point, it is important to mention that Eq. (4) does not imply an internal mass transfer due to diffusion and/or convection mechanisms. A similar approach has been successful used for water and lipid content prediction in contact-heating cooking of hamburgers (Pan et al., 2000) and pan frying of hamburgers (Ou and Mittal, 2006, 2007).

For a given process time t, the evaporative loss (EL) is predicted by surface integration of evaporative mass flux:

$$EL(t) = \int_0^t \left[\int_\Gamma j_{evap}(\Gamma, t) d\Gamma \right] dt \tag{5}$$

As the proposed model does not consider the inner flux of water, the dripping loss at a given process time (DL) is estimated as the difference of liquid water content:

$$DL(t) = m_s(c_i - \bar{C}(t)) \tag{6}$$

where $\bar{C}$ is the volume average moisture content, obtained by volume integration of the moisture profile.

$$\bar{C}(t) = \frac{1}{V} \int_\Omega c(\Omega, t) d\Omega \tag{7}$$

Finally, the total weight loss is obtained by summing both evaporative and dripping losses.

2.1. Thermophysical properties

For the case of study, thermophysical properties of meat were computed according to moisture content (in wet basis, c_{wb}) and temperature, considering only water and proteins as major

components. Properties of individual components were determined according to Choi and Okos (1986). Thermal conductivity was considered to be anisotropic, and the parallel (Eq. (9)) and the perpendicular (Eq. (10)) values were computed from the volumetric fraction of components.

$$\phi_w = \frac{c_{wb}\rho}{\rho_w(T)} \tag{8}$$

$$k_{\parallel} = \phi_w k_w(T) + (1-\phi_w)k_p(T) \tag{9}$$

$$\frac{1}{k_{\perp}} = \frac{\phi_w}{k_w(T)} + \frac{1-\phi_w}{k_p(T)} \tag{10}$$

$$C_P = c_{wb}C_{P,w}(T) + (1-c_{wb})C_{P,p}(T) \tag{11}$$

$$\frac{1}{\rho} = \frac{c_{wb}}{\rho_w(T)} + \frac{(1-c_{wb})}{\rho_p(T)} \tag{12}$$

Beef emissivity, which appears in the energy boundary condition (Eq. (2)), was considered equal to 0.9 (Townsend et al., 1989a). Water activity at beef surface, needed to evaluate evaporative flux (Eq. (3)), was expressed according to van der Sman (2007a,b):

$$a_w = 1 - \frac{0.08}{c} \tag{13}$$

3. Materials and methods

3.1. Samples and cooking tests

Six cooking tests were performed to validate the proposed mathematical model, where thermal histories, cooking time, weight loss (with evaporative and dripping contributions), and shrinkage were determined. Half pieces of *semitendinosus* muscle (from 0.5 to 1 kg) acquired at local markets were used to perform the experiments. Prior to cooking, superficial fat was removed. Then, the samples were packaged and stored at room or refrigeration temperature during several hours to ensure uniform initial temperature. Initial moisture content of samples was determined according to AOAC official method 950.46 (AOAC, 1995).

Cooking of each sample was performed in a domestic electrical oven (ARISTON FM87-FC, Italy), using the forced convection heating mode and setting a different oven temperature for each piece (detailed in Table 1). Meat (at least surface and core) and oven temperature profiles were measured using T-type thermocouples (Omega, USA) connected to a data logger (Keithley-DASTC, USA). Thermocouples were located before cooking, and then the sample was placed on a coarse netting tray in the central region of the oven. Then, with the sample ready to cook, the oven was turned on. Each experiment was finished, and the corresponding process time was determined, when the core temperature reached 72 °C, since this condition is required for microbiological safety of processed meat products (McDonald et al., 2001). Also, this internal temperature corresponds to "medium" degree of doneness, according to the *Beef Steak Color Guide* (AMSA, 1995, cited by López Osornio et al. (2008)).

To quantify shrinkage during cooking, initial and final characteristic dimensions, i.e. length, width, and height, of samples were measured by using a calliper. In order to calculate total weight loss, the samples were weighed before and after cooking. Furthermore, we experimentally attempted to determine the evaporative and dripping contributions to total weight loss. For this aim, an ad hoc procedure was performed for each cooking test (see Fig. 1):

1. A roasting pan with a known mass of water is placed underneath the tray with the sample, at the bottom of the oven. In this way, any amount of water expelled from the meat is collected (note that the use of an empty pan would lead to rapid evaporation of the dripped water). Previous experiments are done to determine the necessary quantity of water to prevent its complete evaporation in the pan.
2. During cooking, the pan collects the dripped liquid from meat which is weighed at the end of the cooking test.
3. In an independent experiment but under the same operating conditions as cooking test, only the pan with liquid water is placed in the oven and the weight variation is registered.
4. The dripping loss during meat cooking can be calculated by the weight difference of both pans (i.e. with and without the sample being cooked).
5. Finally, evaporative loss can be estimated by difference between total weight and dripping losses.

3.2. Water holding capacity and K_W estimation

The water holding capacity (*WHC*) describes the ability of meat to resist the removal of liquid that could result from squeezing the beef or from gravity (Bengtsson et al., 1976). In our case, it was desired to determine this capacity as a function of temperature, in the absence of water evaporation. So, water holding capacity of samples was measured according to Bengtsson et al. (1976). Thin slices of meat (3–4 mm thickness) were packaged into plastic pouches and immersed in a thermostatic bath using different combinations of time (from 2.5 to 30 min) and bath temperature (from 40 to

Table 1
Sample characteristics and experimental results of the cooking tests.

Sample	#1	#2	#3	#4	#5	#6
Initial weight (kg)	1.0799	0.7406	0.9718	0.6325	0.4900	0.7795
Initial water content	2.65	2.97	3.31	3.09	2.72	3.64
Initial T (°C)	20.63	13.30	7.50	12.95	7.00	15.34
T_o, at regime (°C)	212.89	223.50	185.41	193.80	197.26	172.83
Cooking time (min)	87.50	75.00	91.50	74.00	63.00	78.50
Weight loss (kg)						
Total	0.4068	0.2276	0.2674	0.1679	0.1135	0.2081
Evaporative	0.2358	0.1154	0.1214	0.0785	0.0338	0.1042
Dripping	0.1710	0.1122	0.1460	0.0894	0.0797	0.1039
Shrinkage, initial and (final) characteristic dimensions (cm)						
Height	8.2 (8.5)	7.3 (8.2)	7.7 (8.1)	6.5 (7.1)	5.7 (6.4)	6.7 (7.5)
Width	10.6 (8.0)	10.0 (8.0)	10.5 (8.0)	8.5 (7.6)	9.0 (7.5)	11.2 (9.3)
Length	17.7 (14.6)	15.7 (12.2)	17.5 (13.9)	14.0 (11.5)	13.0 (10.7)	14.3 (11.3)
Geometric modelling						
No. of slices	10	10	8	8	9	8
Average thickness (cm)	15.2	12.2	16.3	14.5	11.2	14.4

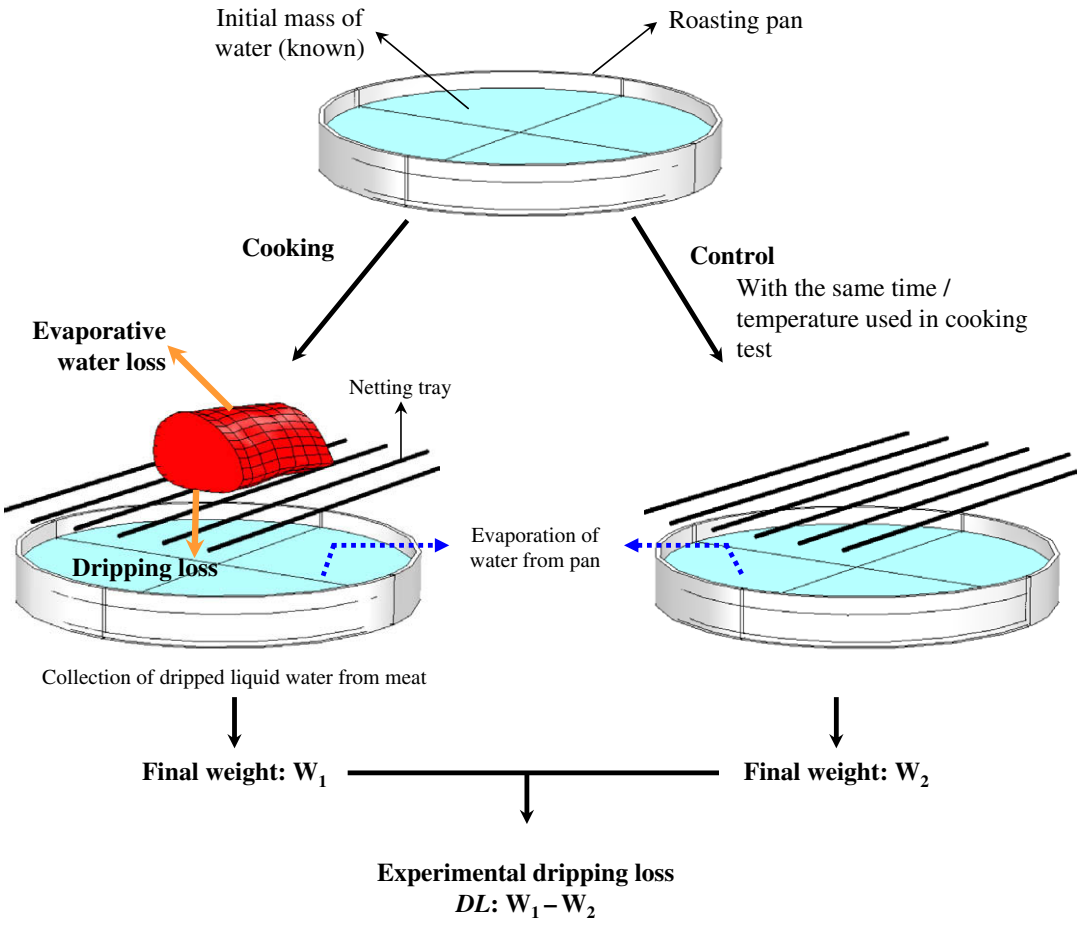

Fig. 1. Schematic representation of experimental procedure used to estimate dripping and evaporative contribution to total weight loss.

100 °C). After the thermal treatment, samples were blotted for 1 min using absorbent paper towels at room temperature. At each temperature, water content was then obtained by weighing the sample; the final value (at 30 min) was defined as *WHC*. These data were fitted to a sigmoid function (van der Sman, 2007a,b):

$$WHC(T) = c_i - \frac{a_1}{1 + a_2 \exp(a_3(T - T_R))} \quad (14)$$

where c_i is the initial moisture content of raw sample. The unknown parameters of Eq. (14), i.e. a_1, a_2, a_3, T_R, were estimated by non-linear regression using the Levenberg–Marquardt method.

In addition, the experimental values of water content variation were used to estimate the parameter K_W, which is required to solve the mass balance (Eq. (4)). In order to analyze the dependence of K_W with temperature, we assumed that the sample temperature quickly reaches the water bath temperature, i.e. isothermal condition, which is actually true for a thin slice of meat. Then, the value of K_W can be calculated by means of the analytical solution of Eq. (4):

$$c(t) = WHC(T) + (c_i - WHC(T)) \times \exp\left(-\frac{K_W(T)}{m_s}t\right) \quad (15)$$

3.3. Heat and mass transfer coefficients

The convective heat transfer coefficient was estimated from known relationships of Nusselt (*Nu*) vs. Reynolds (*Re*) and Prandtl (*Pr*) dimensionless numbers, for the corresponding experimental cooking conditions. For this aim, the following considerations were done: (i) the meat sample is resembled to a finite cylinder with an equivalent diameter, equal to the average value between the width and height of the raw sample; (ii) thermophysical properties of air are evaluated at an average temperature between the ambient and surface values, once the oven reached a regime condition.

The air velocity inside the oven was measured using a hot wire anemometer (Solomat MPM2000, United Kingdom). The velocity measured in the central region of the oven ($v = 0.85$ m s^{-1}) was used to evaluate the *Re* number, which indicated that forced convection cooking mode was used. Under this condition, Eq. (15) was used (Perry and Green, 1997) to determine the convective heat transfer coefficient:

$$Nu = 0.683 Re^{0.466} Pr^{1/3}, \quad 40 \leq Re \leq 4000 \quad (16)$$

The mass transfer coefficient was then estimated by using a heat-mass transfer analogy (Obuz et al., 2002). This approach, similar to the Chilton–Colburn's analogy, relates both convective transfer coefficients:

$$k_g = \frac{h}{64.7\lambda} \quad (17)$$

3.4. Geometric modelling

Beef samples were considered as three-dimensional solid objects having an irregular shape for simulation purposes. In order to obtain the geometrical representation of each sample, the following procedure was performed:

a. After cooking, the sample was packaged and cooled at 4 °C during several hours; then, it was sliced along the axial axis,

and a digital image (in RGB format) of each slice was obtained using a computer vision system, i.e. a digital camera (Professional Series Network IP Camera, Intellinet Active Networking, USA) connected to a PC.

b. Image processing was performed to obtain the irregular boundary of slices, following several sub-steps:
   1. Conversion of original RGB images to grey-scale format.
   2. Noise reduction by filtering to enhance image quality (optional).
   3. Segmentation through a threshold value which was obtained from the grey-scale image histogram. A binary image is obtained where black color (pixel value equal to 0) represented the background and white color the sample (pixel value equal to 1).
   4. Boundary detection and interpolation of a subset of boundary pixels by a closed B-Spline curve (a continuous approximation to the discrete boundary of binary images).

The obtained B-Spline curves approximating the real boundaries of slices were assembled by means of a lofting technique in COMSOL™ Multiphysics (COMSOL AB, Sweden) and MATLAB. In this way, a closed surface is obtained, which was then transformed in a 3D solid object. For further details about the developed procedure to perform geometric modelling, the reader should be referred to Goñi et al. (2007, 2008a).

Note that the geometric models were obtained from the cooked samples, which were actually different from the raw pieces since a significant volume change (i.e. shrinkage) occurred during the process. However, the geometric model of the raw sample is required for modelling and simulation purposes. So, such model was obtained by scaling the former, using three scaling factors calculated as the ratio between raw and cooked characteristic dimensions of sample, i.e. length, width and height.

3.5. Numerical solution

Simulation of meat cooking model (Eqs. (1)–(7)) was performed by using the finite element method implemented in COMSOL™ Multiphysics. Initial uniform temperature and moisture content were considered for all simulations (obtained from experimental measurements). For each sample, the corresponding geometric model and the experimental profiles recorded during the cooking tests were used.

A mesh consisting of ca. 6400 (in average) deformed tetrahedrons was used. The solver used is an implicit variable time-stepping scheme combined with Newton's method to solve the resulting non-linear equation system. Simulation time was fixed to 10 min more than experimental cooking times; solution time was about 2–3 min using a PC with a 1.86 GHz Intel Core^{2}Duo Processor and 3.25 GB RAM.

The goodness of all fitting procedures as well as the simulated temperature profiles were assessed by means of the absolute average relative deviations (Eq. (18)), where n is the size of data set.

$$AARD = \frac{100}{n}\sum_{i=1}^{n}\left|\frac{value_{sim} - value_{exp}}{value_{exp}}\right| \quad (18)$$

4. Results and discussion

4.1. Cooking tests

4.1.1. Temperature profiles

Fig. 2a shows a sample inside the oven with inserted thermocouples, where also the pan used to measure the dripped water during cooking can be seen, while Fig. 2b shows a slice of cooked beef, indicating the positions where the thermocouples were inserted. In this way, Fig. 3 illustrates two representative temperature profiles obtained during cooking tests. Note that the oven temperature profile presents a delay (~15 to 30 min) before reaching the selected oven temperature. This is due to experimental procedure adopted (see Section 3.1). After this warm-up period, the oven automatically controls the set value with an accuracy of ±5 °C.

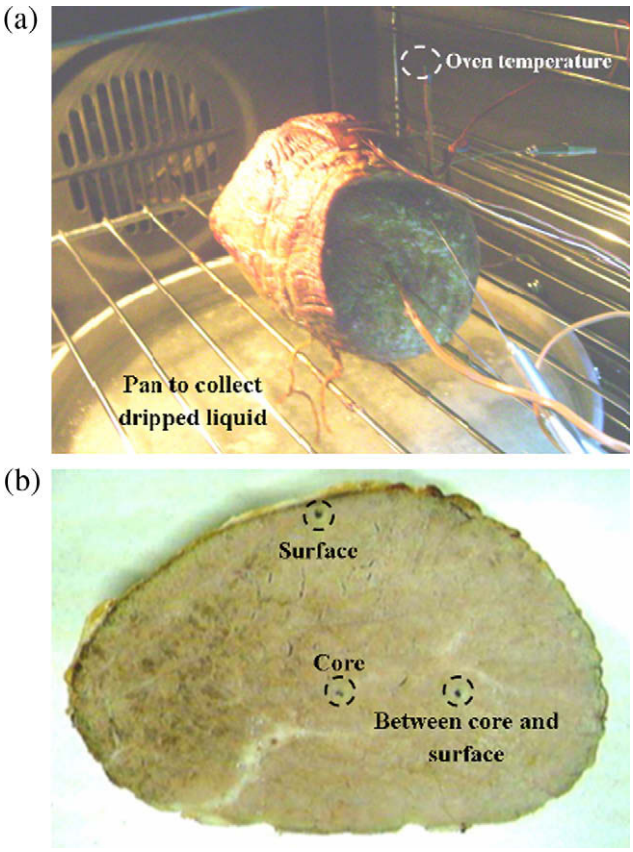

Fig. 2. (a) Experimental setup. (b) Thermocouple locations.

Respect to meat results, in all cases the lowest temperature corresponded to the core, and the highest to the surface. At long process times, a plateau ca. 100 °C was observed for surface temperature. This behaviour can be correlated with a constant (or near constant) drying rate period, in which the surface is sufficiently wet and water evaporation takes place, therefore limiting a temperature increase. Furthermore, the evaporative front is maintained near the surface, avoiding the formation of a crust (i.e. dehydrated outer layer). This observation can be verified through Fig. 2b, where only a thin darker (mainly due to browning reactions) layer is visualized, mostly in the upper regions. Other researchers found similar behaviour during meat cooking in domestic ovens (Bengtsson et al., 1976; Singh et al., 1984; Obuz et al., 2002). Finally, Table 1 summarizes the cooking times for all tested conditions. It is worth to note that actual cooking times could be slightly different from the experimental ones due to the difficult task of exactly locating a thermocouple at the sample core, especially for irregular shaped materials suffering volume change during the process. The oven temperature values shown in Table 1 correspond to the average value once the oven reaches the regime.

4.1.2. Weight loss

The initial water content, raw weight and weight loss for all samples are detailed in Table 1, and Fig. 4 shows the total weight

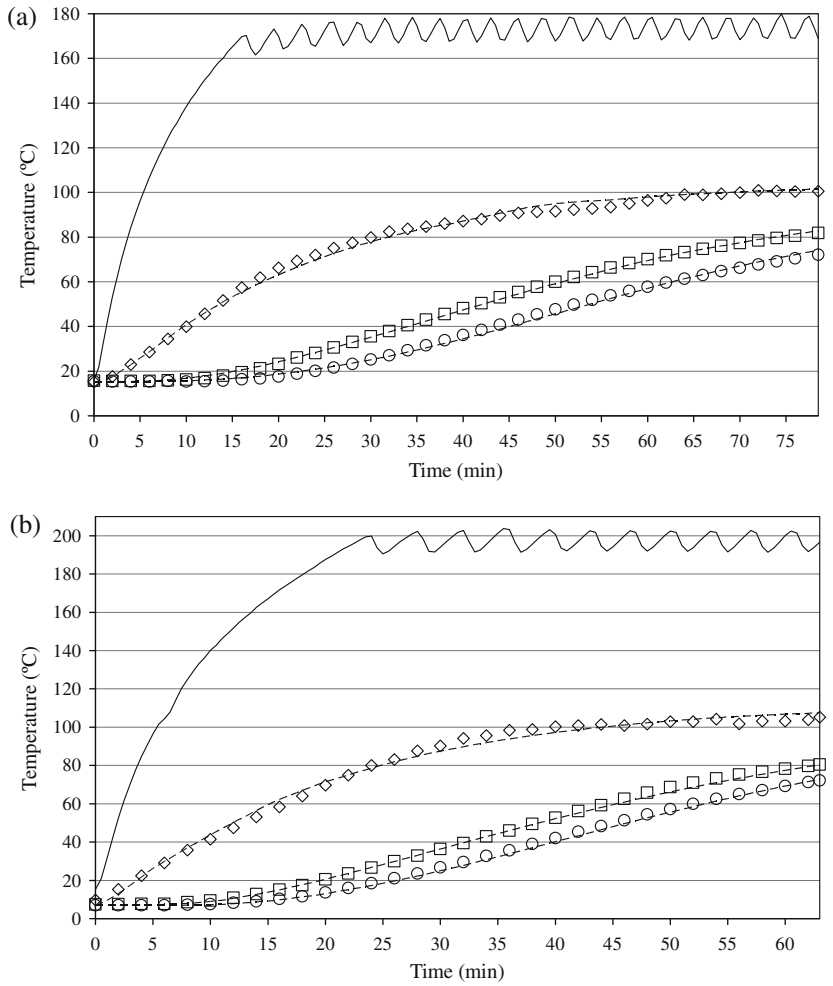

Fig. 3. Measured temperatures: (○) core; (◇) surface; (□) between core and surface. (a) Sample #6. (b) Sample #5. Continuous line is oven temperature. Dashed lines are the model prediction for the same locations.

loss and the contribution of both evaporative and dripping mechanisms (respect to raw weight). Average total weight loss was 28.72%. Based on measured values, it can be say that dripping is very important in the tested operative conditions, since its contribution is of the same order of evaporative losses. In average, 53.22% of the total weight loss was produced by dripping; a similar value is reported by Bengtsson et al. (1976). Moreover, a tendency for the contribution of each mechanism to weight loss could be established respect to product size: for small samples (i.e. 0.5–0.7 kg initial weight), dripping would be the responsible for most of weight loss, while for large samples (>1 kg initial weight) evaporation would dominate. In addition, big pieces of meat seem to suffer more weight reduction than small ones. Further analysis and experiments are needed to explain the contribution of different mechanisms of weight loss as a function of sample size.

During the cooking tests, an interesting phenomenon was observed: liquid water expelled from meat by dripping remained "adsorbed" to the surface until large droplets were formed; at this point, water was allowed to flow down to lower regions of the beef and finally to oven bottom (where the pan with water was placed; see Section 3.1). This behaviour surely depends on the gravitational force and the surface tension that the droplet must support and overcome, as well as the viscosity of the dripped fluid. In consequence, a fraction of the dripped water was evaporated at the surface, so the obtained experimental values for dripping contribution are probably lower than the actual ones.

4.1.3. Sample size variation

Characteristic dimensions measured before and after cooking are summarized in Table 1. In all cases, it was found that the final height was greater than the initial one, with an average size ratio (i.e. cooked/raw value) of 109.11% (SD 3.83%), while the width and length of the sample were reduced, with an average size ratio of 81.24% (SD 5.19%) and 80.52% (SD 2.05%), respectively. Similar results were also reported by other authors (Godsalve et al., 1977; van der Sman, 2007b).

4.2. Water holding capacity and K_W estimation

Fig. 5a shows the variation of water content of meat samples measured during the experiments described in Section 3.2. As it was expected, water content diminished as temperature increased. The moisture value obtained at long immersion time (i.e. 30 min heating) for each temperature was defined as *WHC*. In this way, as the temperature increased, the ability of meat to retain water was reduced, which is due to thermal protein denaturation. Subsequently, the experimental values of *WHC* (as a function of temperature) were fitted to Eq. (14). Firstly, the parameter a_1 was set to $(c_i - 0.961)$ kg water/kg dry solid, since a final moisture content or *WHC* of 0.961 (in average) was obtained for high temperature (100 °C) independently of initial water content of samples. Then, the following values for other parameters of Eq. (14) were found by regression: $a_2 = 3.2674$; $a_3 = -9.0027 \times 10^{-2}$ °C^{-1}; $T_R = 48.27$ °C. Fig. 5b shows

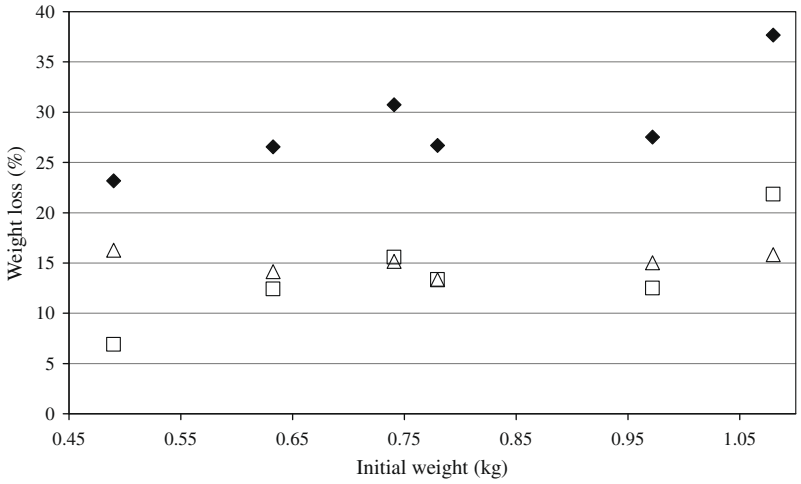

Fig. 4. Total percentage weight loss (♦) and the contribution of both evaporative (□) and dripping (△) mechanism (respect to raw weight).

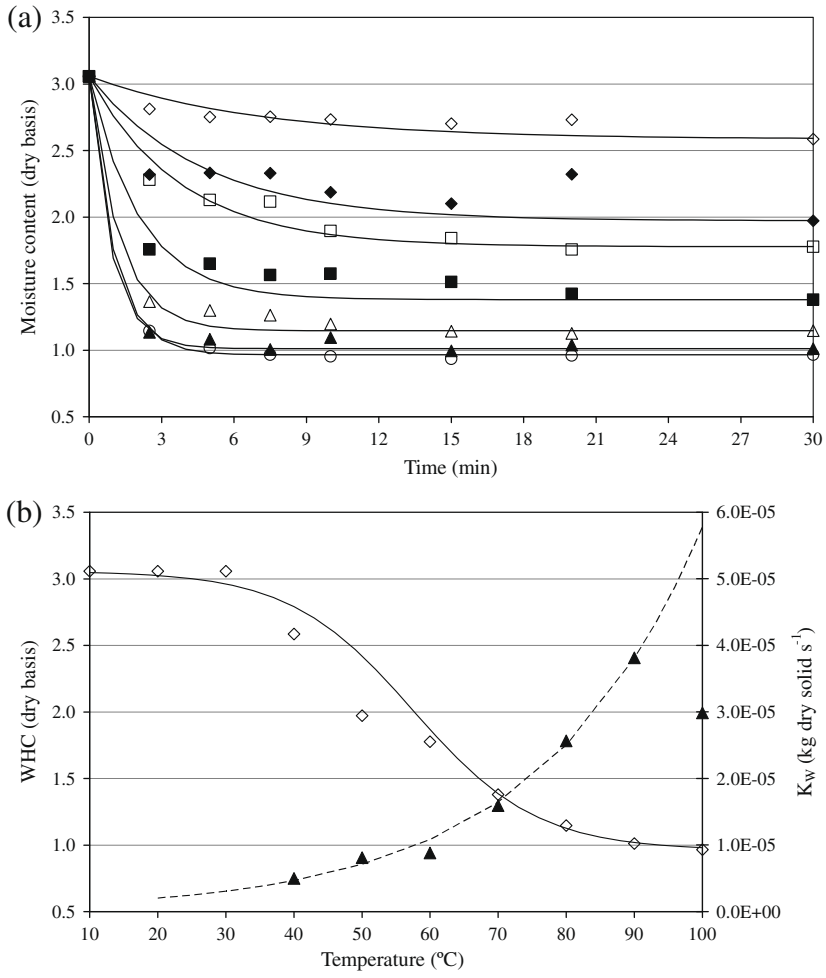

Fig. 5. (a) Experimental (symbols) water content variation and fit of Eq. (15) (lines) at different water bath temperatures: (◇) 40 °C; (♦) 50 °C; (□) 60 °C; (■) 70 °C; (△) 80 °C; (▲) 90 °C; (○) 100 °C. (b) Values of water holding capacity (◇) and fit of Eq. (14) (continuous line); K_W parameter (▲) and fit of Eq. (19) (dashed line).

the experimental *WHC* data and the corresponding fitted sigmoid expression, which have an AARD of 4.10%.

Data of water content as a function of time were used to estimate the parameter K_W for each tested temperature, through Eq. (15). The performance of parameter estimation is shown in Fig. 5a, besides the AARD was found to be 3.18%. Furthermore, we analyzed the dependence of K_W with temperature (Fig. 5b). With the aim of using this parameter in the mathematical model for roasting, the following expression was proposed to describe its dependence with temperature:

$$K_W(T) = 4.669 \times 10^{-6} \exp(4.495 \times 10^{-2} (T - 40)) \quad (19)$$

Note that Eq. (19) was obtained by neglecting the data corresponding to 100 °C, since the K_W value for this temperature should be at least equal to the one at 90 °C. We attribute these results to estimation of K_W by using all data of water content as a function of time. At high temperatures (80–100 °C), the equilibrium condition (*WHC*) was achieved rapidly, i.e. all variation was observed before 10 min (Fig. 5a). In this way, the sensitivity of Eq. (15) is low for long times and high uncertainty is related to estimation of K_W at high temperature.

4.3. Geometric modelling

Fig. 6 illustrates the developed geometric modelling procedure for a representative sample. As can be seen, the obtained geometric model is in good agreement with the shape of the actual raw sample. Table 1 details the number of slices and the average slice thickness used for each beef sample. Fig. 7 shows the meshed geometric models for the six samples used to validate the developed mathematical model.

In order to perform an objective evaluation of this procedure, the volume of the cooked samples, measured by liquid displacement method, was compared with the volume calculated from the constructed geometric models (before scaling), according to Goñi et al. (2007). The AARD between both values was 3.90% (equivalent to 18.26 cm^3). Additionally, the density of the samples was determined by using the measured initial weight and the estimated volume of raw sample (from geometric models after scaling); an average density of 1064.3 kg m^{-3} was calculated. This value agrees with the one calculated from both experimental weight and volume, i.e. 1065 kg m^{-3}. Therefore, the presented procedure demonstrated its ability to accurately reproduce the shape of the samples.

4.4. Numerical simulation of cooking

Numerical simulation of meat cooking was performed by using the finite element method. Each experimental condition was represented by the corresponding values of transfer coefficients, being the average values of heat and mass transfer coefficients 9.676 W m^{-2} °C^{-1} (SD 0.456) and 6.502×10^{-8} kg Pa^{-1} m^{-2} s^{-1} (SD 3.669×10^{-9}), respectively. The goodness of the developed model was evaluated by comparing the experimental and simulated thermal histories at surface and core (coldest point), the cooking time, and the weight loss of the samples.

Fig. 3 shows the evolution of both experimental and simulated temperature profiles at three internal positions for two different beef samples. As can be seen, the model well describes the temperature variation in all positions. The values of AARD for core and surface temperature profiles as well as experimental and predicted cooking times are detailed in Table 2. In general terms, simulated core temperature is slightly higher than experimental one, producing a small under–prediction of the process time, equivalent to 3.17 min, in average; the AARD for this parameter was 3.91%. Fig. 8 shows the simulated temperature and water content profiles for a whole sample (#3), at a specific time (40 min).

Regarding the weight loss, Table 3 shows the measured and predicted values for all beef samples. The predicted total weight loss, obtained from Eqs. (5) and (6), presented an AARD equal to 7.96%, equivalent to 0.0152 kg. This result is a good indicator that the

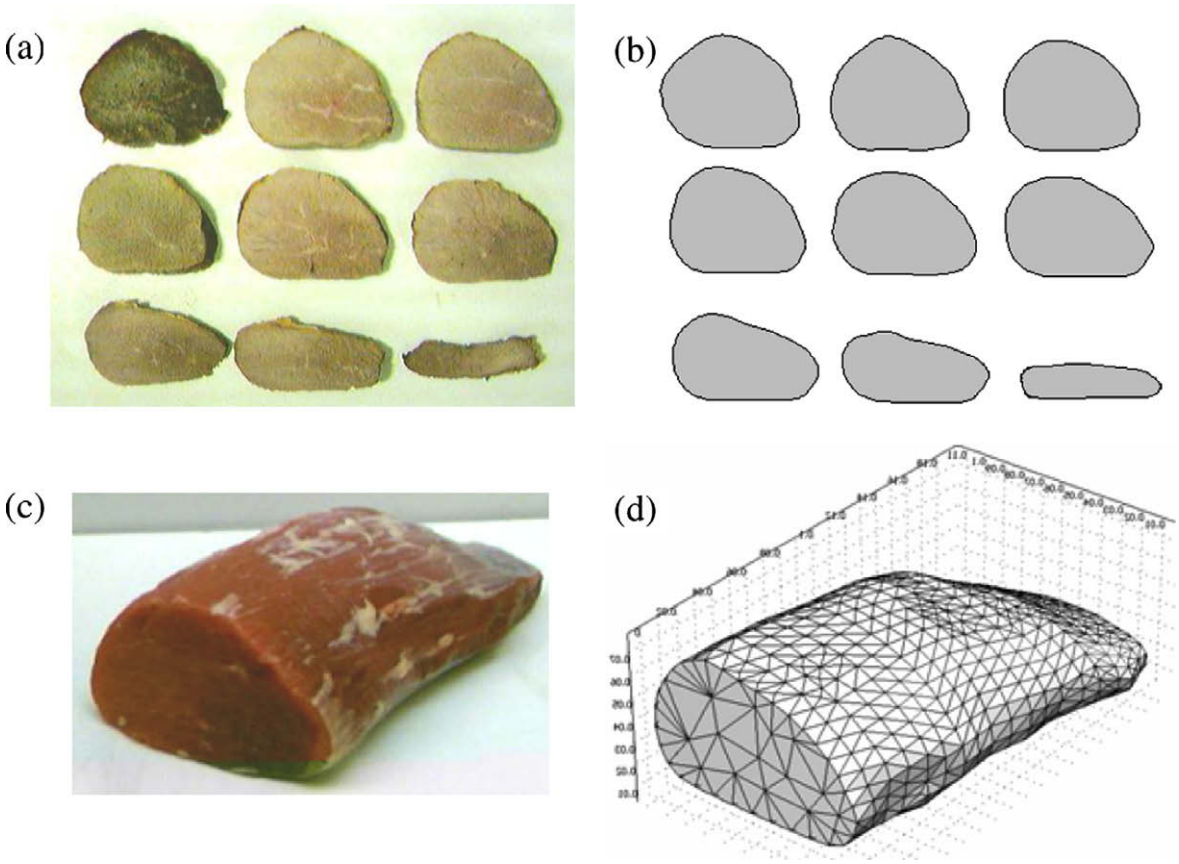

Fig. 6. (a) Original images used to construct the geometric model. (b) Result of applying the procedure to approximate the shape of each slice. (c) Image of whole raw sample and (d) constructed geometric model (which is already scaled to raw sample dimensions and meshed).

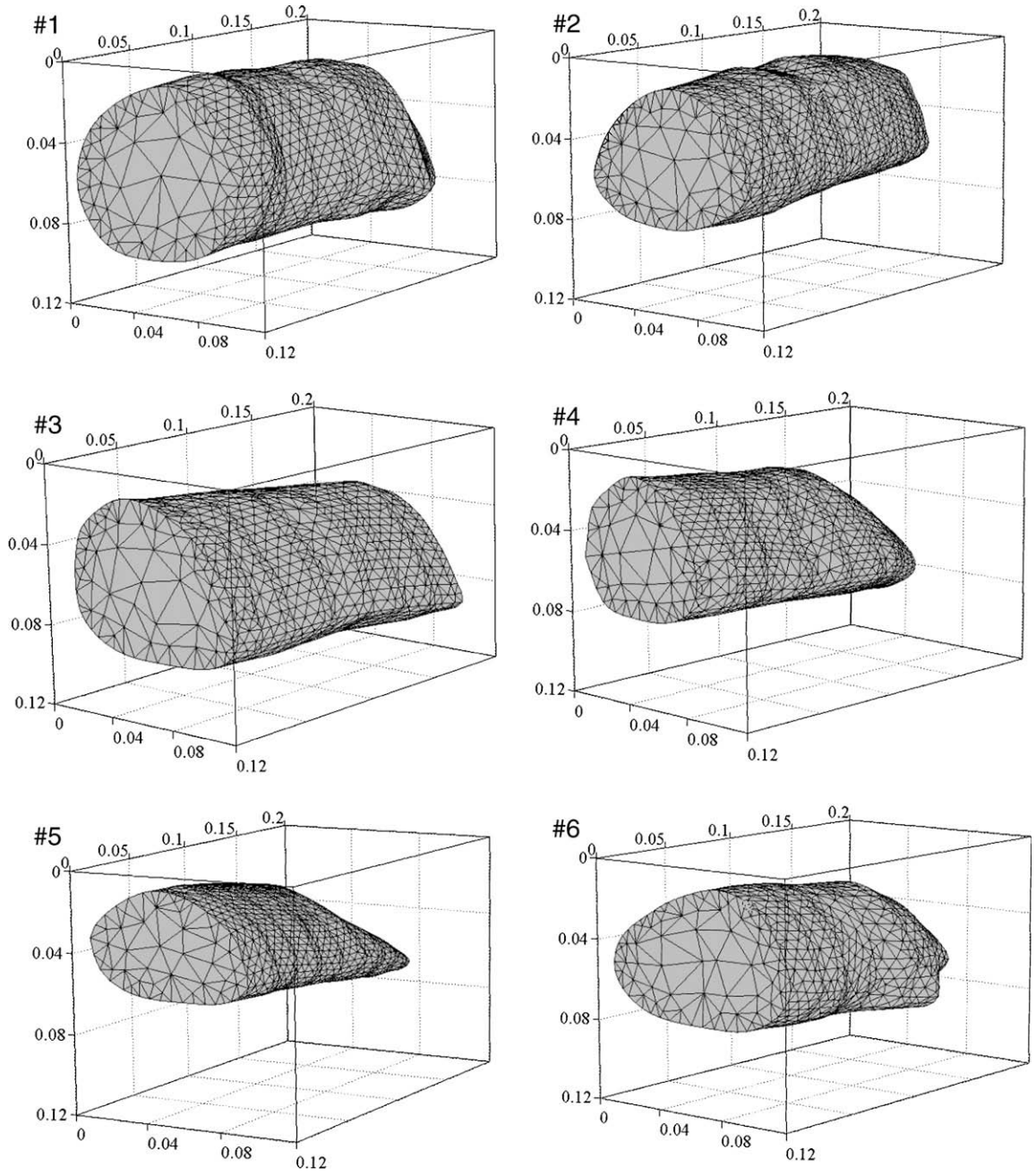

Fig. 7. Meshed geometric models for the six samples used in experimental determinations and model simulations. The geometric models are already scaled to raw dimensions.

proposed model is accurately representing the water loss occurring during the used cooking conditions.

Table 2
Measured and predicted cooking times and temperature profiles error.

Sample	Cooking time (min)		AARD (%)	
	Measured	Predicted	Core	Surface
#1	87.50	82.50	2.93	1.73
#2	75.00	71.50	3.90	5.39
#3	91.50	87.50	3.10	5.98
#4	74.00	70.50	3.84	2.06
#5	63.00	62.50	3.63	5.32
#6	78.50	76.00	2.74	1.78

Respect to individual contributions, AARD for dripping and evaporative losses were equal to 21.71% and 26.44%, respectively. Furthermore, simulated dripping contribution to total weight loss was 55.21% (average value), a similar value to the experimental one reported in Section 4.1.2. Respect to these high AARD values, it is important to remark at this instance that the proposed cooking model allows the prediction of each contribution to total weight loss, representing a significant advance in beef cooking modelling.

At this instance, it is important to mention that the parameter K_W, required to solve the proposed mathematical model, can be determined by means of a simple experimental procedure, i.e. it does not imply its estimation through the solution of an inverse problem.

Finally, it is worth to note that the use of high realistic representation of the sample reduces the geometry influences on the

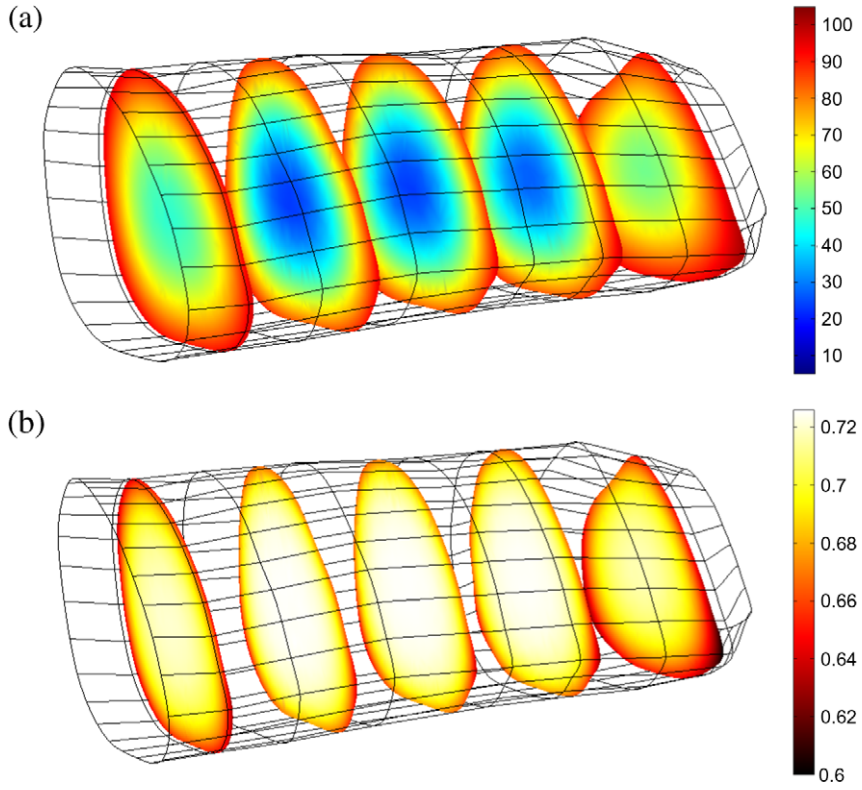

Fig. 8. Simulated profiles of (a) temperature (°C) and (b) water content (wet basis), at 40 min cooking for the sample #3.

Table 3
Measured and predicted weight loss with evaporative and dripping contributions.

Sample	Measured weight loss (kg)			Predicted weight loss (kg)		
	Total	Evaporative	Dripping	Total	Evaporative	Dripping
#1	0.4068	0.2358	0.1710	0.3963	0.1928	0.2035
#2	0.2276	0.1154	0.1122	0.2531	0.1257	0.1274
#3	0.2674	0.1214	0.1460	0.2610	0.1191	0.1419
#4	0.1679	0.0785	0.0894	0.1915	0.0783	0.1132
#5	0.1135	0.0338	0.0797	0.1270	0.0663	0.0607
#6	0.2081	0.1042	0.1039	0.2197	0.0696	0.1501

simulated results, and we can focus on the error associated with model assumptions and development.

5. Conclusions

In this work, a simultaneous heat and mass transfer model to simulate meat oven cooking is proposed and accordingly validated. The model describes internal heat transfer by Fourier's law and the concept of water demand (related to the water holding capacity of meat) is used to describe the inner water content variation during the process. Bearing in mind the ultimate objective of our work, i.e. multi-objective optimization of roasting, the model is focused on predicting cooking time and weight loss. In this way, two mechanisms of water loss are incorporated: evaporation and dripping. Through experimental data, it is demonstrated that the approach adopted well described such a complex process, including both temperature and weight loss variations.

In order to reduce errors associated to experimental measurement of variables such as temperature and water content, realistic geometric models are used. It is shown that this methodology helps to improve the model predictions as well as not increasing the computational cost of simulations. Finally, the developed model appears as a valuable tool to optimize and control the oven cooking (or roasting) of beef.

Acknowledgments

We thank Dr. Emmanuel Purlis for helpful comments during the development of this work. Authors acknowledge Consejo Nacional de Investigaciones Científicas y Técnicas (CONICET), Agencia Nacional de Promoción Científica y Tecnológica (ANPCyT 2007-01090), and Universidad Nacional de La Plata (UNLP, 11I140) from Argentina for their financial support.

References

American Meat Science Association, 1995. Research Guidelines for Cookery, Sensory Evaluation and Instrumental Tenderness Measurements of Fresh Meat. National Live Stock and Meat Board, Chicago.
AOAC, 1995. In: Helrich, K. (Ed.), Official Methods of Analysis of the Association of Official Analytical Chemists, fifth ed. AOAC, Washington, DC.
Bengtsson, N.E., Jakobsson, B., Dagerskog, M., 1976. Cooking of beef by oven roasting: a study of heat and mass transfer. Journal of Food Science 41 (5), 1047–1053.
Bottani, E., Volpi, A., 2009. An analytical model for cooking automation in industrial steam ovens. Journal of Food Engineering 90 (2), 153–160.
Burfoot, D., Self, K.P., 1989. Predicting the heating times of beef joints. Journal of Food Engineering 9 (4), 251–274.
Chang, H.C., Carpenter, J.A., Toledo, R.T., 1998. Modeling heat transfer during oven roasting of unstuffed turkeys. Journal of Food Science 63 (2), 257–261.
Chen, H., Marks, B.P., Murphy, R.Y., 1999. Modeling coupled heat and mass transfer for convection cooking of chicken patties. Journal of Food Engineering 42 (3), 139–146.
Choi, Y., Okos, M.R., 1986. Effects of temperature and composition on the thermal properties of foods. In: Le Maguer, M., Jelen, P. (Eds.), Food Engineering and Process Applications: Transport Phenomena. Elsevier Applied Science, Amsterdam.
COMSOL AB. COMSOL Multiphysics User's Guide. Version: September 2005, COMSOL 3.2.

Godsalve, E.W., Davis, E.A., Gordon, J., Davis, H.T., 1977. Water loss rates and temperature profiles of dry cooked bovine muscle. Journal of Food Science 42 (4), 1038–1045.

Goñi, S.M., Purlis, E., Salvadori, V.O., 2007. Three-dimensional reconstruction of irregular foodstuffs. Journal of Food Engineering 82 (4), 536–547.

Goñi, S.M., Purlis, E., Salvadori, V.O., 2008a. Geometry modelling of food materials from magnetic resonance imaging. Journal of Food Engineering 88 (4), 561–567.

Goñi, S.M., Purlis, E., Salvadori, V.O., 2008b. Evaluating a simple model for meat cooking simulation. In: Proceedings of CIGR 2008 – International Conference of Agricultural Engineering – XXXVII Congresso Brasileiro de Engenharia Agrícola, Iguassu Falls City, Brazil.

Huang, E., Mittal, G.S., 1995. Meatball cooking – modeling and simulation. Journal of Food Engineering 24 (1), 87–100.

López Osornio, M.M., Hough, G., Salvador, A., Chambers IV, E., McGraw, S., Fiszman, S., 2008. Beef's optimum internal cooking temperature as seen by consumers from different countries using survival analysis statistics. Food Quality and Preference 19, 12–20.

McDonald, K., Sun, D.-W., Kenny, T., 2001. The effect of injection level on the quality of a rapid vacuum cooled cooked beef product. Journal of Food Engineering 47 (2), 139–147.

Obuz, E., Powell, T.H., Dikeman, M.E., 2002. Simulation of cooking cylindrical beef roasts. Lebensmittel-Wissenschaft und-Technologie 35 (8), 637–644.

Obuz, E., Dikeman, M.E., Erickson, L.E., Hunt, M.C., Herald, T.J., 2004. Predicting temperature profiles to determine degree of doneness for beef *biceps femoris* and *longissimus lumborum* steaks. Meat Science 67 (1), 101–105.

Ou, D., Mittal, G.S., 2006. Double-sided pan frying of unfrozen/frozen hamburgers for microbial safety using modelling and simulation. Food Research International 39, 33–45.

Ou, D., Mittal, G.S., 2007. Single-sided pan frying of frozen hamburgers with flippings for microbial safety using modeling and simulation. Journal of Food Engineering 80 (1), 33–45.

Pan, Z., Singh, R.P., Rumsey, T.R., 2000. Predictive modeling of contact-heating for cooking a hamburger patty. Journal of Food Engineering 46 (1), 9–19.

Perry, R.H., Green, D.W., 1997. Perry's Chemical Engineers' Handbook, seventh ed. McGraw-Hill, New York.

Singh, N., Akins, R.G., Erickson, L.E., 1984. Modeling heat and mass transfer during the oven roasting of meat. Journal of Food Process Engineering 7 (3), 205–220.

Tornberg, E., 2005. Effects of heat on meat proteins – implications on structure and quality of meat products. Journal of Food Engineering 70 (3), 493–508.

Townsend, M.A., Gupta, S., Pitts, W.H., 1989a. The roast: nonlinear modeling and simulation. Journal of Food Process Engineering 11 (1), 17–42.

Townsend, M.A., Gupta, S., Pitts, W.H., 1989b. Optimal roasting. Journal of Food Process Engineering 11 (2), 117–145.

van der Sman, R.G.M., 2007a. Moisture transport during cooking of meat: an analysis based on Flory–Rehner theory. Meat Science 76 (4), 730–738.

van der Sman, R.G.M., 2007b. Soft condensed matter perspective on moisture transport in cooking meat. American Institute of Chemical Engineers 53 (11), 2986–2995.